Optical Engineering

SPIEDigitalLibrary.org/oe

Improved maximum likelihood detection for mitigating fading estimation error in free space optical communication

Lu Zhang
Zhiyong Wu
Yaoyu Zhang
Huang Detian

Improved maximum likelihood detection for mitigating fading estimation error in free space optical communication

Lu Zhang
Chinese Academy of Sciences
Changchun Institute of Optics
Fine Mechanics and Physics
Changchun, Dong-Nanhu Road 3888
Jilin 130033, China
and
Graduate University of Chinese Academy of Sciences
Beijing 10049, China
E-mail: LZhangpai@gmail.com

Zhiyong Wu
Yaoyu Zhang
Chinese Academy of Sciences
Changchun Institute of Optics
Fine Mechanics and Physics
Changchun, Dong-Nanhu Road 3888
Jilin 130033, China

Huang Detian
Chinese Academy of Sciences
Changchun Institute of Optics
Fine Mechanics and Physics
Changchun, Dong-Nanhu Road 3888
Jilin 130033, China
and
Graduate University of Chinese Academy of Sciences
Beijing 10049, China

Abstract. To mitigate the impact of the error between the estimated channel fading coefficient and the perfect fading coefficient on the bit error rate (BER), *a priori* conditional probability density function averaging the estimation error is proposed. Then, an improved maximum-likelihood (ML) symbol-by-symbol detection is derived for the free-space optical communication systems, which implement pilot symbol assisted modulation. To reduce complexity, a closed-form suboptimal improved ML detection is deduced using distribution approximation. Numerical results confirm that BER performance improvement can be reached by the improved ML detection, and that its suboptimal version performs as well as it does. Therefore, they both outperform classical ML detection, which doses not consider channel estimation error. © *2013 Society of Photo-Optical Instrumentation Engineers (SPIE).* [DOI: 10.1117/1.OE.52.1.015004]

Subject terms: improved maximum-likelihood detection; channel estimation error; pilot symbol; free-space optical communication.

Paper 121312 received Sep. 11, 2012; revised manuscript received Nov. 22, 2012; accepted for publication Dec. 4, 2012; published online Jan. 7, 2013.

1 Introduction

Free-space optical (FSO) systems operating over a turbulent atmosphere channel experience fading of the received optical signal, which severely affect the reliability of the FSO link. Currently, the on-off keying (OOK) intensity modulation (IM) and direct detection (DD) are mainly employed for commercial FSO systems. For such mechanisms, the perfect channel's instantaneous fading intensity is needed to detect the received fading signal. Many previous studies assumed the receiver had perfect knowledge of the instantaneous fading intensity.[1–4] To avoid dependency on the perfect instantaneous fading intensity, detection techniques without channel state information (CSI) have attracted attention. Zhu and Kahn[5–7] first investigated maximum-likelihood sequence detection (MLSD) in the context of FSO communications. Despite MLSD's efficiency, the computation of multidimensional integrals are inevitable for MLSD, therefore it suffers from high complexity.[8–10] To reduce the complexity, suboptimal MLSD metrics have been proposed in Refs. 8 and 9 for different detection models. Similarly, to address the complexity issue and to get rid of the dependent on channel's fading statistics, another generalized maximum-likelihood sequence detection (GMLSD) suboptimal detection rule has been suggested in Ref. 10. But in practical implementation, GMLSD requires at least one symbol in the transmitted sequence to correspond to the on-state. Though the above multi-symbol detection methods do not require the perfect knowledge of the instantaneous fading intensity, it brings out severe delay and high complexity. In practical systems, pilot symbol assisted modulation (PSAM) has been shown to be an effective solution for obtaining channel state information at the receiver (CSIR).[11] For PSAM, some known pilot symbols were sent,[12–14] then the receiver estimated the instantaneous fading intensity before proceeding to the detection of data symbols. However, due to the finite length of pilot symbols and to noise, the receiver just obtains an imperfect estimation of the channel,[11] so the detection performance is greatly degraded.

To mitigate the impact of the error induced by the imperfect channel estimation, in this paper, an improved ML symbol-by-symbol detection and its suboptimal version are deduced for an FSO system, which implements PSAM and operates over atmospheric turbulence induced fading channel.

0091-3286/2013/$25.00 © 2013 SPIE

2 Signal Model

In this section, we list the channel fading model of interest and introduce the received signal model.

2.1 *Channel Fading Model*

An FSO system employing IM/DD and OOK modulation is considered. For weak turbulence channel, the logarithm of the intensity variations is normally distributed and the probability density function (pdf) of I is given by Refs. 8–10

$$p_I(I) = \frac{1}{I\sqrt{2\pi\sigma^2}} \exp\left[-\frac{(\ln I + \sigma^2/2)^2}{2\sigma^2}\right], \tag{1}$$

with $\sigma^2 = \ln(\text{S.I.} + 1)$ and S.I. being the scintillation index. Based on Eq. (1), $E\{I\} = 1$ is satisfied.

In moderate turbulence, the channel is considered to be a gamma-gamma fading channel, in which the atmospheric fluctuations are modelled as being gamma-gamma distributed. For gamma-gamma fading, the pdf of the intensity is given by Refs. 8–10

$$p_I(I;\alpha,\beta) = \frac{2(\alpha\beta)^{\frac{\alpha+\beta}{2}}}{\Gamma(\alpha)\Gamma(\beta)} I^{\frac{\alpha+\beta-2}{2}} K_{\alpha-\beta}(2\sqrt{\alpha\beta I}), \tag{2}$$

where $\Gamma(\cdot)$ is the gamma function, $\mathrm{K}_\nu(\cdot)$ is the v'th-order modified Bessel function of the second kind, and α and β are interrelated parameters which directly characterize the effective atmospheric conditions. The scintillation index can be calculated from α and β according to $\text{S.I.} = \alpha^{-1} + \beta^{-1} + (\alpha\beta)^{-1}$.

Lastly, in strong turbulence, a negative exponential fading channel model is considered. The pdf of I is given by[8–10]

$$p_I(I) = \exp\{-I\}, \tag{3}$$

and the scintillation index is equal to unity.

For the signaling rates of interest, i.e., hundreds to thousands of Mbps, the fading intensity I can be treated as constant over the observation window, which means that all of the information-bearing bits in the same observation window experience the same I.

2.2 *Received Signal Model*

A FSO communications system employing IM/DD and OOK modulation is considered. And, it is assumed that the receiver operates in the high signal-to-ratio (SNR) regime. That is, a shot-noise limited model of a high-energy FSO system is considered. Hence, a Gaussian noise model is a good approximation of the Poisson photon counting detection model.[5,8,15] The photodetector in the FSO receiver converts the received optical field to electrical signal, which is proportional to the intensity of the optical field. This electrical signal is integrated over each bit interval to produce a set of statistics suitable for detection. For the k'th bit interval, the received discrete-time signal[2,6,8] is given by

$$r(k) = s(k)I + w(k), \tag{4}$$

with $s(k) \in \{0, 1\}$ being the transmitted OOK symbol, I being the channel fading coefficient due to atmospheric turbulence, and $w(k)$ being the additive white Gaussian noise. The mean and variance of $w(k)$ are 0 and σ_w^2, respectively. Given the transmitted bit $s(k)$ and channel fading coefficient I, the pdf for received bit $r(k)$[6,8,16] is

$$p[r(k)|s(k), I] = \frac{1}{\sqrt{2\pi\sigma_w^2}} \exp\left\{-\frac{[r(k) - s(k)I]^2}{2\sigma_w^2}\right\}. \tag{5}$$

The average SNR[2,6,8] is defined as

$$\gamma \triangleq \frac{E[s(k)I]^2}{E\{[w(k)]^2\}} = \frac{\mu_I^2}{4\sigma_w^2}, \tag{6}$$

where $\mu_I = E\{I\}$ is the mean of the intensity.

3 Pilot Symbol Assisted Maximum-Likelihood Detection

At the receiver end of a FSO system implementing PSAM, to recover the transmitted data from the received statistics, the receiver estimates the channel fading coefficient based on received pilot symbols first, then ML symbol-by-symbol detection can be performed by comparing a received bit to a threshold, precalculated using the estimated channel fading coefficient. However, due to the finite number of pilot symbols and to noise, the receiver only obtains an imperfect estimation of the channel fading coefficient, which induces degradation to the receiver performance. The method we take to mitigate the impact of the estimation error is to design an improved ML receiver, which averages the estimation error. In this section, firstly, we derive the pdf of the estimation error. Then an improved ML symbol-by-symbol detection is derived. Subsequently, its suboptimal version is deduced.

3.1 *Probability Density Function for Estimation Error*

In the k'th observation interval, assuming that the transmitted pilot sequence is $\mathbf{s} = [s(0), \ldots, s(p-1)]$, the corresponding fading coefficient of this interval is I, thus, the received sequence is $\mathbf{r} = \mathbf{s} \cdot I + \mathbf{w}$. To estimate I, the least-squares estimate (LSE) minimizing $\|\mathbf{r} - \mathbf{s} \cdot I\|^2$ with respect to I is used.[17] The LSE yields

$$\hat{I} = \mathbf{r}\mathbf{s}^{\mathrm{T}}(\mathbf{s}\mathbf{s}^{\mathbf{T}})^{-1} = I + \mathbf{w}\mathbf{s}^{\mathrm{T}}(\mathbf{s}\mathbf{s}^{\mathbf{T}})^{-1}, \tag{7}$$

where $\varepsilon = \mathbf{w}\mathbf{s}^{\mathrm{T}}(\mathbf{s}\mathbf{s}^{\mathbf{T}})^{-1}$ is the channel estimation error. Therefore, Eq. (7) can be rewritten as

$$\hat{I} = I + \varepsilon, \tag{8}$$

where $\varepsilon = \mathbf{w}\mathbf{s}^{\mathrm{T}}(\mathbf{s}\mathbf{s}^{\mathbf{T}})^{-1}$ is a zero-mean Gaussian random variable with a variance given by $\sigma_\varepsilon^2 = \sigma_w^2(\mathbf{s}\mathbf{s}^{\mathbf{T}})^{-1}$. From Eq. (8), the conditional pdf of $\hat{I}$ given I, i.e., the pdf for estimation error ε, can be deduced as

$$p(\hat{I}|I) = \frac{1}{\sqrt{2\pi\sigma_\varepsilon^2}} \exp\left[-\frac{(\hat{I} - I)^2}{2\sigma_\varepsilon^2}\right], \tag{9}$$

3.2 *Improved ML Symbol-by-Symbol Detection*

Considering the received signal model in this paper, the likelihood ratio is given by

$$\Lambda[r(k)|I] = \exp\left\{-\frac{[r(k)-I]^2 - r^2}{2\sigma_w^2}\right\}, \tag{10}$$

with I being the instantaneous channel fading coefficient. Using the perfect I, the optimal ML symbol-by-symbol detection can be realized by Eq. (10). However, in practice, a realizable and widely accepted method to obtain the perfect I is channel estimation using the pilot-aided symbols. But there is error between the estimated $\hat{I}$ and perfect I. Replacing I by $\hat{I}$, the ML detection using Eq. (10) leads to BER performance degradation, thereby, the optimal ML detection degrades to suboptimal ML detection. Consequently, the estimation error must be considered. Thus, a new priori conditional pdf for $r(k)$ given $s(k)$ and $\hat{I}$ is defined as

$$p[r(k)|s(k),\hat{I}] = \int_0^\infty p[r(k)|s(k),I]p(\hat{I}|I)p_I(I)\mathrm{d}I, \tag{11}$$

where $p[r(k)|s(k),I)$ is given by Eq. (5), $p(\hat{I}|I)$ is given by Eq. (9), and $p_I(I)$ is the pdf of channel fading coefficient, which may be given by Eqs. (1)–(3).

Based on the new priori conditional pdf, the improved likelihood ratio can be defined as

$$\begin{aligned}\Lambda[r(k)|\hat{I}] &= \frac{p[r(k)|s(k)=1,\hat{I}]}{p[r(k)|s(k)=0,\hat{I}]} \\ &= \frac{\int_0^\infty p[r(k)|s(k)=1,I]p(\hat{I}|I)p_I(I)\mathrm{d}I}{\int_0^\infty p[r(k)|s(k)=0,I]p(\hat{I}|I)p_I(I)\mathrm{d}I}.\end{aligned} \tag{12}$$

Thereby, the improved ML symbol-by-symbol detection can be performed by comparing the improved likelihood ratio $\Lambda[r(k)|\hat{I}]$ with 1. However, due to the complex form of $p_I(I)$, it is difficult to obtain the closed-form expression for Eqs. (11) and (12), so single integral has to be computed, which increases the complexity.

3.3 *Suboptimal Improved ML Symbol-by-Symbol Detection*

Due to the mathematically intricate and specialized nature of the fading intensity pdf in a FSO system,[8] generalized closed-form expressions for Eqs. (11) and (12) prove to be intractable. In this subsection, using a distribution approximation, generalized analytical expressions for Eqs. (11) and (12) are derived.

In Ref. 8, the fading intensity pdfs in Eqs. (1)–(3) were effectively approximated by an Erlang distribution. The Erlang distribution[8] is given by

$$p_{I,\mathrm{Er}}(I;\theta,\lambda) = \frac{\lambda^\theta}{(\theta-1)!}I^{\theta-1}\exp\{-\lambda I\}, \qquad I \geq 0, \tag{13}$$

where $\theta \in \mathbb{Z}^+$ and $\lambda \in \mathbb{R}$ are the distribution parameters. To determine the parameters θ and λ, a minimum squared error criterion was proposed in Ref. 8, and some parameters were obtained for several specific distributions. Using the Erlang distribution and substituting Eqs. (5) and (9) into Eq. (11), the integral in Eq. (11) becomes

$$\begin{aligned}p_{\mathrm{Er}}[r(k)|s(k),\hat{I}] &= \int_0^\infty p[r(k)|s(k),I]p(\hat{I}|I)p_{I,\mathrm{Er}}(I;\theta,\lambda)\mathrm{d}I \\ &= \frac{\lambda^\theta}{(\theta-1)!}\frac{1}{\sqrt{2\pi\sigma_\varepsilon^2}}\exp\left\{-\frac{1}{2}\left[\frac{r(k)^2}{\sigma_w^2}+\frac{\hat{I}^2}{\sigma_\varepsilon^2}\right]\right\} \\ &\quad\times\int_0^\infty I^{\theta-1}\exp\left(-\left\{\left[\frac{s(k)^2\sigma_\varepsilon^2+\sigma_w^2}{2\sigma_w^2\sigma_\varepsilon^2}\right]I^2\right.\right. \\ &\quad\left.\left.+\left[\lambda-\frac{s(k)r(k)}{\sigma_w^2}-\frac{\hat{I}}{\sigma_\varepsilon^2}\right]I\right\}\right)\mathrm{d}I.\end{aligned} \tag{14}$$

Executing the integral in Eq. (11) yields

$$\begin{aligned}p_{\mathrm{Er}}[r(k)|s(k),\hat{I}] &= \frac{1}{\sqrt{2\pi\sigma_\varepsilon^2}}\exp\left\{-\frac{1}{2}\left[\frac{r(k)^2}{\sigma_w^2}+\frac{\hat{I}^2}{\sigma_\varepsilon^2}\right]\right\} \\ &\quad\times\frac{\lambda^\theta}{(\theta-1)!}\frac{\exp\{\nu^2\}}{\mu^{\theta/2}}\frac{\sqrt{\pi}}{2}W_{\theta-1}(\nu),\end{aligned} \tag{15}$$

where

$$\mu = \frac{s(k)^2\sigma_\varepsilon^2+\sigma_w^2}{2\sigma_w^2\sigma_\varepsilon^2}, \tag{16}$$

$$\nu = \left[\lambda-\frac{s(k)r(k)}{\sigma_w^2}-\frac{\hat{I}}{\sigma_\varepsilon^2}\right](2\sqrt{\mu})^{-1}, \tag{17}$$

and

$$W_k(x) \triangleq \frac{2}{\sqrt{\pi}}\int_0^\infty y^k\exp[-(y+x)^2]\mathrm{d}y, \tag{18}$$

is termed the weighted complementary error function (WCEF),[8] valid for integer k and real number x. The detail about WCEF can be found in Ref. 8, where an iteration expression for WCEF has been described. Thus, using the Erlang distributed fading, Eq. (11) has an easily evaluated closed-form expression. As a result, a closed-form expression for Eq. (12) is deduced as

$$\begin{aligned}\Lambda_{\mathrm{Er}}[r(k)|\hat{I}] &= \frac{p_{\mathrm{Er}}[r(k)|s(k)=1,\hat{I}]}{p_{\mathrm{Er}}[r(k)|s(k)=0,\hat{I}]} \\ &= \frac{\exp\{\nu_1^2\}W_{\theta-1}(\nu_1)\mu_0^{\theta/2}}{\mu_1^{\theta/2}\exp\{\nu_0^2\}W_{\theta-1}(\nu_0)},\end{aligned} \tag{19}$$

where

$$\mu_1 = \frac{\sigma_\varepsilon^2+\sigma_w^2}{2\sigma_w^2\sigma_\varepsilon^2}, \tag{20}$$

$$\nu_1 = \left[\lambda-\frac{r(k)}{\sigma_w^2}-\frac{\hat{I}}{\sigma_\varepsilon^2}\right](2\sqrt{\mu_1})^{-1}, \tag{21}$$

and

$$\mu_0 = \frac{1}{2\sigma_\varepsilon^2}, \tag{22}$$

$$\nu_0 = \left(\lambda - \frac{\hat{I}}{\sigma_\varepsilon^2}\right)(2\sqrt{\mu_0})^{-1}. \tag{23}$$

Therefore, suboptimal improved ML symbol-by-symbol detection can be performed using Eq. (19).

For a received symbol sequence with N symbols, Eqs. (20), (22) and (23) are only computed one time. So, in Eq. (19), only the computation of $\exp\{\nu_1^2\}W_{\theta-1}(\nu_1)$ is necessary per symbol. Thus, for sequence with N symbols, $O(N)$ operations are required to compute Eq. (19), and $O(N)$ to perform comparison between Eq. (19) and (1) In summary, our suboptimal improved ML detection algorithm has an overall complexity of $O(N)$ operations per N symbol decisions, and is only linearly dependent on N.

4 Numerical Results

In this section, the Monte-Carlo simulation results for the BER performance of the improved ML detection and its suboptimal version are presented in various turbulence conditions. For reference, the detection with genie bound,[8] given by

$$\mathrm{BER}_{\text{genie bound}} = E_I\left[\frac{1}{2}erfc\left(\frac{I/2}{\sqrt{2\sigma_w^2}}\right)\right], \tag{24}$$

is also included. The parameters for the Erlang distribution corresponding to the considered channel models are given in Ref. 8. In our simulation, we assume that the probability of transmitting symbol '1' equals to that of transmitting symbol '0', i.e., $P_0 = P_1 = 1/2$, and the number of performing Monte-Carlo simulation is 10^6. For lognormal channel, scintillation index S.I. = 0.5 and Erlang distribution parameters $\{\theta, \lambda\} = \{4, 4.474\}$ are used. For gamma-gamma channel, there are S.I. = 0.88 and $\{\theta, \lambda\} = \{2, 2.368\}$. As well S.I. = 1 and $\{\theta, \lambda\} = \{1, 1\}$ are used for negative exponential channel. In addition, without loss of generality, $\mu_I = E\{I\} = 1$ is assumed in our simulation. In the following tables, 'PS-Length' means the length of pilot symbols, 'SNR-I' is SNR achieved by improved ML receiver, 'SNR-S' is SNR reached by classically suboptimal ML receiver, and ΔSNR = SNR-S − SNR-I.

In Fig. 1, an FSO communication system operating over lognormal fading channel (S.I. = 0.5) is considered. The BER performance of the improved ML receiver and classically suboptimal ML receiver are compared. From Fig. 1 and Table 1, it can be observed that for $N = 1$, the improvement in terms of required SNR to reach a given BER is about 1 dB when SNR ≥ 8 dB, it is about 0.7 dB when SNR < 8 dB, compared with the classically suboptimal ML receiver which is realized by replacing I by $\hat{I}$ in Eq. (10). For $N = 4$, the improvements are all about 0.5 dB. It is obvious that these improvements are reduced when increasing the pilot symbols' length. Furthermore, the BER performance reached by the improved ML receiver is closer to genie bound than that reached by the suboptimal ML receiver for the same pilot symbols length. Besides, we place special emphasis on that the BER performance of the improved ML receiver with 1 pilot symbol ($N = 1$) is very close to that of the suboptimal ML receiver with four pilot symbols ($N = 4$). Thus, the improved ML receiver with one pilot symbol can achieve higher rates than the classically suboptimal ML receiver with four pilot symbols.

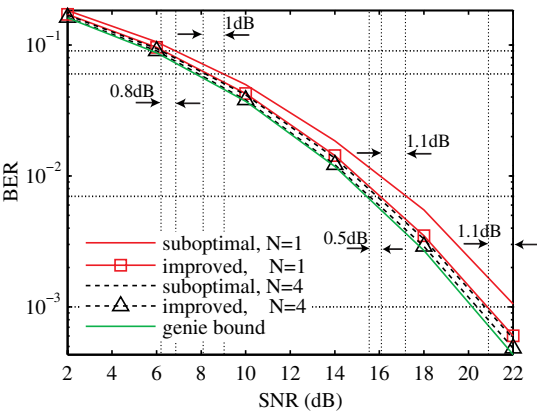

Fig. 1 Bit error rate (BER) performance of the improved maximum likelihood (ML) receiver Eq. (12), classically suboptimal ML receiver Eq. (10), where I is replaced by $\hat{I}$, and the classically optimal ML receiver with genie bound for a lognormal fading channel: S.I. = 0.5. SNR = Signal to noise ratio.

Table 1 SNR achieved by improved ML receiver and classically suboptimal ML receiver at given BER for lognormal fading channel: S.I. = 0.5.

PS-Length	BER	SNR-I (dB)	SNR-S (dB)	ΔSNR (dB)
$N = 1$	10^{-3}	20.9	22.0	1.1
	7×10^{-3}	16.0	17.1	1.1
	6×10^{-2}	8.0	9.0	1.0
	9×10^{-2}	6.1	6.9	0.8
$N = 4$	7×10^{-3}	15.6	16.1	0.5

Similar results are shown in Figs. 2 and 3 for the case of gamma-gamma fading channel (S.I. = 0.88) and negative exponential fading channel (S.I. = 1), respectively. Seen from Tables 2 and 3, for $N = 1$, the improvement in terms of required SNR to reach a given BER is also about 1 dB when SNR ≥ 8 dB, it is about 0.7 dB when SNR < 8 dB, compared with the classically suboptimal ML receiver, which is implemented by replacing I by $\hat{I}$ in Eq. (10). Clearly, the BER performance of the improved ML receiver with one pilot symbol ($N = 1$) in Figs. 2 and 3 are much closer to genie bound than that of the improved ML receiver with one pilot symbol in Fig. 1. But compared with the BER performance of Fig. 1, due to the increase of turbulence strength, the BER in Figs. 2 and 3 are larger.

The BER performance results of the suboptimal improved ML receiver implemented by Eq. (19) for lognormal fading ("LOG"), gamma-gamma fading ("GA") and negative exponential fading ("NE") are given in Fig. 4. For comparison, the BER performance of the corresponding improved ML receivers is also included. It can be observed that there is

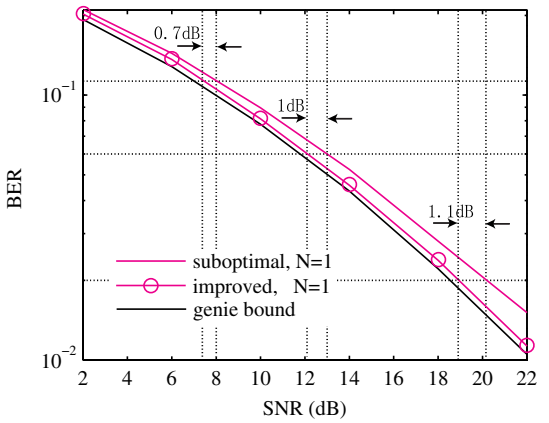

Fig. 2 Bit error rate (BER) performance of the improved maximum likelihood (ML) receiver Eq. (12), classically suboptimal ML receiver Eq. (10), where I is replaced by $\hat{I}$, and the classically optimal ML receiver with genie bound for a gamma-gamma fading channel: $\alpha = 4$, $\beta = 2$, S.I. = 0.88. SNR = Signal to noise ratio.

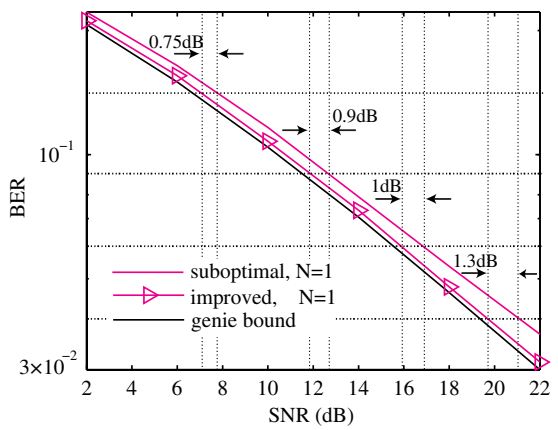

Fig. 3 Bit error rate (BER) performance of the improved maximum likelihood (ML) receiver Eq. (12), classically suboptimal ML receiver Eq. (10), where I is replaced by $\hat{I}$, and the classically optimal ML receiver with genie bound for a negative exponential fading channel: S.I. = 1. SNR = Signal to noise ratio.

Table 2 SNR achieved by improved ML receiver and classically suboptimal ML receiver at given BER for gamma-gamma fading channel: S.I. = 0.88.

PS-Length	BER	SNR-I (dB)	SNR-S (dB)	ΔSNR (dB)
$N = 1$	2×10^{-2}	18.95	20.05	1.1
	6×10^{-2}	12.0	13.0	1.0
	1.2×10^{-1}	7.3	8.0	0.7

good agreement between BER performance achieved by the improved ML receivers and that achieved by their suboptimal versions. It indicates that the suboptimal improved ML receiver degrades the BER performance lightly. But due to its low-complexity, the suboptimal improved ML detection is a good alternative for improved ML detection implemented by Eq. (12).

Table 3 SNR achieved by improved ML receiver and classically suboptimal ML receiver at given BER for negative exponential fading channel: S.I. = 1.

PS-Length	BER	SNR-I (dB)	SNR-S (dB)	ΔSNR (dB)
$N = 1$	4×10^{-2}	19.7	21.0	1.3
	6×10^{-2}	16.0	17.0	1.0
	9×10^{-2}	11.9	12.8	0.9
	1.4×10^{-1}	7.1	7.85	0.75

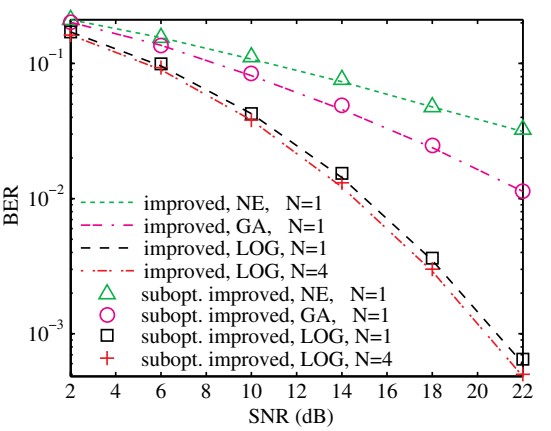

Fig. 4 Comparison of the bit error rate (BER) performance of the improved maximum likelihood (ML) receiver Eq. (12) and its suboptimal version Eq. (19) for lognormal fading channel (S.I. = 0.5), gamma-gamma fading channel (S.I. = 0.88) and negative exponential fading channel (S.I. = 1). SNR = Signal to noise ratio.

5 Conclusions

In this paper, *a priori* conditional pdf for received signal, which averages the estimation error, is proposed to mitigate the impact of the error between the estimated channel fading coefficient and the perfect fading coefficient on BER. Using the priori conditional pdf, an improved likelihood ratio is derived. Therefore, an improved ML symbol-by-symbol detection becomes available. To reduce complexity, a closed-form expression of the likelihood ratio for the improved ML detection is deduced, which results in the suboptimal improved ML detection. Simulation results indicate that rates increase and BER performance improvement can be reached by the improved ML detection. As well, the suboptimal improved ML detection agrees with the improved ML detection well in terms of BER performance. Hence, they both outperform classical ML detection, which doses not consider channel estimation error. Finally, the impact of the error between the estimated fading coefficient and the perfect one on the BER has been mitigated.

Acknowledgments

This work has been carried out with the financial support of the Innovation Project of Chinese Academy of Sciences (Y10532B110).

References

1. M. Uysal, S. M. Navidpour, and J. Li, "Error rate performance of coded free-space optical links over strong turbulence channels," *IEEE Commun. Lett.* **8**(10), 635–637 (2004).
2. M. K. Simon and V. A. Vilnrotter, "Alamouti-type space-time coding for free-space optical communication with direct detection," *IEEE Trans. Wireless Commun.* **4**(1), 35–39 (2005).
3. M. Jazayerifar and J. A. Salehi, "Atmospheric optical CDMA communication systems via optical orthogonal codes," *IEEE Trans. Commun.* **54**(9), 1614–1623 (2006).
4. M. Uysal, J. Li, and M. Yu, "Error rate performance analysis of coded free-space optical links over gamma-gamma atmospheric turbulence channels," *IEEE Trans. Wireless Commun.* **5**(6), 1229–1233 (2006).
5. X. Zhu and J. M. Kahn, "Pilot-symbol assisted modulation for correlated turbulent free-space optical channels," *Proc. SPIE* **4489**, 138–145 (2001).
6. X. Zhu and J. M. Kahn, "Free-space optical communication through atmospheric turbulence channels," *IEEE Trans. Commun.* **50**(8), 1293–1300 (2002).
7. X. Zhu and J. M. Kahn, "Markov chain model in maximum-likelihood sequence detection for free-space optical communication through atmospheric turbulence channels," *IEEE Trans. Commun.* **51**(3), 509–516 (2003).
8. M. L. B. Riediger, R. Schober, and L. Lampe, "Fast multiple-symbol detection for free-space optical communications," *IEEE Trans. Commun.* **57**(4), 1119–1128 (2009).
9. M. L. B. Riediger, R. Schober, and L. Lampe, "Multiple-symbol detection for photon-counting MIMO free-space optical communications," *IEEE Trans. Wireless Commun.* **7**(12), 5369–5379 (2008).
10. N. D. Chatzidiamantis, G. K. Karagiannidis, and M. Uysal, "Generalized Maximum-Likelihood sequence detection for photon-counting free space optical systems," *IEEE Trans. Commun.* **58**(12), 3381–3385 (2010).
11. S. M. S. Sadough and P. Duhamel, "Improved iterative detection and achieved throughputs of OFDM systems under imperfect channel estimation," *IEEE Trans. Wireless Commun.* **7**(12), 5039–5050 (2008).
12. H. Moradi, H. H. Refai, and P. G. LoPresti, "Thresholding-based optimal detection of wireless optical signals," *J. Opt. Commun. Netw.* **2**(9), 689–700 (2010).
13. H. Moradi et al., "A PSAM-based estimator of noise and fading statistics for optimum receivers of free space optics signals," *Proc. SPIE* **7587**, 75870O (2010).
14. M. Cole and K. Kiasaleh, "Receiver architectures for the detection of spatially correlated optical field using avalanche photodiode detector arrays," *Opt. Eng.* **47**(2), 025008 (2008).
15. H. R. Burris et al, "A comparison of adaptive methods for optimal thresholding for free-space optical communication receivers with multiplicative noise," *Proc. SPIE* **4821**, 139–154 (2002).
16. N. D. Chatzidiamantis et al., "Interative near maximum-likelihood sequence detection for MIMO optical wireless systems," *J. Lightwave Technol.* **28**(7), 1064–1070 (2010).
17. B. C. Levy, "Linear least-squares estimation," in *Principles of Signal Detection and Parameter Estimation: Parameter Estimation Theory*, pp. 125–130, Springer Science+Business Media LLC, New York (2008).

Lu Zhang received his BS in electrical engineering from Northeast Normal University, Changchun, China, in 2008. He is currently a PhD student in circuits and systems at Changchun Institute of Optics, Fine Mechanics and Physics, Chinese Academy of Sciences. His current research interests include fiber optics, wireless optical communications, laser beam propagation in atmospheric turbulence, and optical coherent detection.

Zhiyong Wu received his BS in electronics engineering from Changchun University of Science and Technology, Changchun, China, in 1989. He is currently a professor in Circuits and Systems at Changchun Institute of Optics, Fine Mechanics and Physics, Chinese Academy of Sciences. His current research interests include laser ranging, free-space optical communications, and EO theodolite.

Yaoyu Zhang received his BS in mechanical engineering from Jilin University in 1996. In 2003, he received a PhD degree in mechanics and electronics engineering from Changchun Institute of Optics, Fine Mechanics and Physics, Chinese Academy of Sciences (CIOMP). He is currently a professor in Optical Engineering at CIOMP and an assistant director at Optoelectronic Measuring and Controlling Technology Laboratory. His current research interests include Optoelectronic Measuring and Controlling Technology, and EO theodolite.

Huang Detian received a BS from Xiamen University in 2008. Now, he is a PhD student in Changchun Institute of Optics, Fine Mechanics and Physics, Chinese Academy of Sciences. His research interests are image enhancement, image restoration, and auto-focusing.